

Optimizing Energy Spread in the CLIC Main Linac

G. Guignard and C. Fischer
CERN, 1211 Geneva 23, Switzerland

Abstract

Making a final focus system of possible linear colliders accept the beam energy spread is an important problem. The feasibility of a certain compensation of the energy spread in a linac has already been established. This paper describes a systematic study leading to rigorous compensation of the longitudinal wake fields with the RF sinusoidal wave, using the CLIC main-linac parameters. The dependence of the energy spread on the RF voltage phase, bunch intensity and bunch length is discussed. Code parts have been written to compute the resulting energy distribution, average energy and energy spread in each case considered. Conditions were found that allow minimal tail population and somewhat narrow core size, so that at the optimum the energy spread is below 10^{-3} for $5 \cdot 10^9$ particles and satisfies final focus requirements. A new set of parameters more favourable to the CLIC performance and solving the problem initially addressed can be drawn out of the results.

I INTRODUCTION AND BASIC PRINCIPLES

The possibility of compensating the energy spread in the CLIC linac using wake potential versus RF wave has already been considered [1]. This paper reports on a systematic study of a cancellation to high orders of the longitudinal wake fields with the RF gradient [2]. Such compensation affects the energy distribution as shown for instance in ref. [3]. Proper adjustments minimize tail population and core size and make the beam's energy spread compatible with final focus acceptance, limited by the radiation in the weak dipoles as well as the sextupole strengths.

Assuming an energy E_{in} and a relative energy spread $g(z)$ at linac entrance, the increase due to an accelerating gradient G is

$$E(z,s) = E_{in} \left[1 + g(z) + \frac{G(z)s}{E_{in}/e} \right] \quad (1)$$

if G is the same all along the linac. The total accelerating gradient seen by a particle at position z results from the RF field diminished by the longitudinal wake, i.e.

$$G(z) = G_{RF} \cos \left(2\pi f_{RF} \frac{z}{c} - \phi_{RF} \right) - W_L(z) \quad (2)$$

where G_{RF} , f_{RF} and ϕ_{RF} are the maximum gradient, frequency and phase of the RF wave. The longitudinal wake is given by the integral

$$W_L(z) = eN \int_{-\infty}^z \rho(z') W_L^\delta(z-z') dz' \quad (3)$$

where the functions under the integration sign are the charge distribution, assumed to be gaussian with r.m.s. σ_z , and the

wake delta-function due to a charge at z' , ahead of the probe-particle ($z' \leq z$). N is the number of particles in the bunch and σ_z the bunch length.

The energy distribution $v(E)$ has to be calculated in order to study its properties and dependence on parameters such as G_{RF} , ϕ_{RF} , σ_z , and N , and comes from

$$v(E) = \frac{1}{N} \frac{dN}{dE} = \frac{1}{N} \frac{dN}{dz} \frac{dz}{dE} = \frac{\rho(z)}{dE/dz} \quad (4)$$

In principle, the derivative dE/dz can be deduced from (1). In practice, numerical estimates of it are preferred to analytical derivation. It is noticeable however that $v(E)$ becomes infinite when dE/dz vanishes and this is a source of numerical inaccuracies. Once the function $v(E)$ is known, the average energy $\langle E \rangle$ and the r.m.s energy spread σ_E are easily computable from the standard integrals. This has been done for the CLIC main linac, with systematic variations of the main parameters and search for optimum conditions.

II ENERGY DISTRIBUTION PROCESSING

Equ. [4] is used to evaluate the energy distribution $v(E)$. The wake field in $G(z)$ and hence $E(z)$ cannot be described analytically very easily and a numerical approach is preferred (section I). A detailed description of this treatment can be found in ref. [2]; basic steps are now summarized. A gaussian longitudinal bunch distribution $\rho(z)$ considered between $\pm 4\sigma_z$, and divided into M slices or superparticles is handled under the influence of continuous external focusing, RF gradient and wake field using program LINBUNCH [4]; quantities $E(z)$, and $\rho(z)$ used in Equ. (4) are provided for each superparticle of index m ($1 \leq m \leq M$); the longitudinal coordinate z is then replaced by m and Equ. (4) becomes:

$$v(E, m) = \bar{\rho}(m) \bullet \Delta z / [E(m+1) - E(m)] \quad (5)$$

with $\Delta z = 8\sigma_z/M$.

The distribution $E(m)$ is not monotonic, as will be discussed later, and regions of same energy domain (four when the actual gradient presents two maxima) must be recombined to get a unique figure $v(E)$ between E and $E+dE$. In these regions, the initial energy bin distribution is different: the bins $E(m+1) - E(m)$ all have different lengths, the cutting being linear along z and not in the energy domain due to the shape of the accelerating gradient; overlapping regions are therefore reshuffled into identical bin configuration before their merging is performed; the finest bin distribution found among overlapping regions is selected to rearrange the other ones. A monotonic variation $v(E)$ is then obtained [each pair $v(m)$, $E(m)$ being unique] - examples are presented and discussed thereafter and in ref. [2]. The curves are not strictly distributions as the final energy bins do not have the same width.

Statistics: Other quantities of interest such as the norm, the average energy $\langle E \rangle$ and the r.m.s. energy spread $\sigma_E/\langle E \rangle$ can then be processed on the distribution $v(E)$, tailored according to various criteria which can be an energy threshold or a given part of the longitudinal bunch distribution selected specifying a number of r.m.s. values (σ_z).

Quality estimate: From Equ. [4] it is clear that if the distribution $\rho(z)$ is normalized to 1, this remains valid for $v(E)$ in the absence of cut; moreover after cuts at $\pm 1\sigma_z, \pm 2\sigma_z$ the norm values of $v(E)$ can be compared to the expected ones (0.6826, 0.9546); this norm evaluation is performed on $v(E)$ before and after the recombination process previously described; careful averaging between adjacent bins and optimization of the superparticle number M are proceeded with until the expected norm value is reached within a few 10^{-3} .

Table 1 gives some figures for cuts at $\pm 1\sigma_z, \pm 2\sigma_z$ and $\pm 4\sigma_z$, and $M = 701$. The resulting values of $\langle E \rangle$ (normalized to the RF voltage) and $\sigma_E/\langle E \rangle$ are incorporated.

	N1(*)	N2(**)	$\langle E \rangle$	$\sigma_E/\langle E \rangle$ (%)	LINBUNCH	
					$\langle E \rangle$	$\sigma_E/\langle E \rangle$ (%)
$\pm 1\sigma_z$	1.0029	0.6810	.9758	.1602	.976	.156
$\pm 2\sigma_z$	1.0029	0.9554	.9731	.5655	.973	.568
$\pm 4\sigma_z$	1.0029	1.0007	.9717	.9408	.972	.944

(*) before rearrangement and with no cut

(**) after rearrangement

Table 1: Norm values, $\langle E \rangle$ and $\sigma_E/\langle E \rangle$ for $M = 701$

$\langle E \rangle$ and $\sigma_E/\langle E \rangle$ are also processed by LINBUNCH from the distributions $\rho(z)$, $E(z)$ and a further consistency check is possible. Data from LINBUNCH are included for comparison.

III DEPENDENCE ON RELEVANT PARAMETERS

When the RF phase varies for previous nominal values of σ_z and N (0.2 mm and $5 \cdot 10^9$) the average energy is maximum when the bunch is in phase with the RF voltage ($\phi_{RF} = 0$) but the energy spread is not optimized (Fig.1). For the complete distribution ($\pm 4\sigma_z$) a minimum is clearly defined near $\phi_{RF} = 4^\circ$ which moves slightly upwards when cuts are performed as the energy distribution is not symmetrical with z .

The electric field acting on the bunch depends on ϕ_{RF} ; for small values, the head (which does not experience wake fields) sees higher gradients but wakes are stronger on the rest of the bunch, lowering the resulting electric field accordingly. The best balance is for values between 4° and 6° depending on the z domain selected and corresponds to a minimum r.m.s. energy spread (Fig. 1). The bunch energy distribution shows a sharp peak at maximum energy within about 1 per mil and a very long tail; increasing the RF phase up to 6° displaces the peak towards $\langle E \rangle$ but this does not reduce the spread as the tail becomes more populated; the best compromise is for $\phi_{RF} = 4^\circ$ when the full distribution is considered; when it is cut through, the tail is reduced accordingly and the peak moves

towards the origin ($\langle E \rangle$) (Fig. 4). The average energy is then increased as already pointed out (Fig.1).

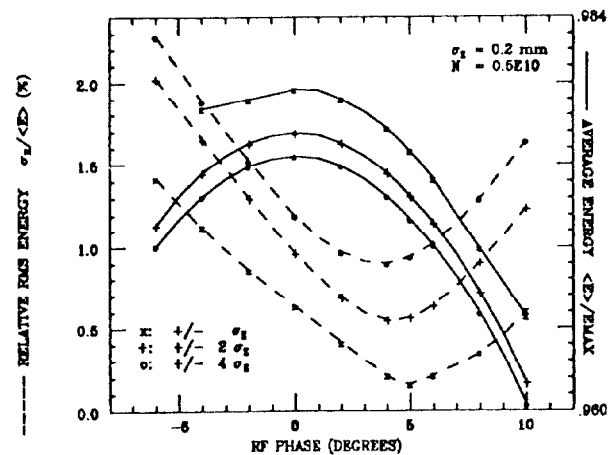


Figure 1. Dependence on RF phase of average energy and energy spread

In order to modify the energy distribution towards a denser core, the curve $G(z)$ should be as flat as possible, likely with two local maxima. Such shapes are obtained by varying the bunch length and/or the number of particles, the RF phase being an adjustment parameter. Starting with $N = 5 \cdot 10^9$ and $\sigma_z = 0.2$ mm this is illustrated in Figs. 2 and 3. Fig. 2 shows the results obtained by shortening the bunch at $\phi_{RF} = 8^\circ$ and constant intensity. Fig. 3 gives curves associated with an increasing charge N , at $\phi_{RF} = 8.5^\circ$ and constant bunch-length. Hence the dense part of the charge distribution is centred around the average energy. However, N and σ_z are linked, in the search for a minimum of σ_E , and both must be decreased simultaneously while the fine tuning of ϕ_{RF} is small. At $N = 5 \cdot 10^9$ the optimum exists for $\sigma_z = 0.14$ mm and $\phi_{RF} = 7^\circ$ giving a σ_E of $\sim 0.5\%$, instead of 1% with 0.2 mm and 5° . Similarly, energy-spread optima exist for each value of N . In such optimized situations, the interesting σ_E - values are those obtained after cutting the energy distribution (lower bound at -4%) according to final focus (FF) acceptance and the number of particles that do not contribute to the luminosity is also minimized (Table 2).

$N (10^9)$	σ_z (mm)	ϕ_{RF}	Fraction lost (%)	$\sigma_E/\langle E \rangle$ (%)
4	0.11	7	4.5	0.156
5	0.14	7	7.7	0.157
6	0.17	8	15.1	0.097
7	0.20	8,5	22.2	0.104

Table 2: Energy spread for various parameters

Table 2 shows that the change in ϕ_{RF} for different charges is not large. However, the fraction of non-contributing particles for an FF acceptance of $\pm 4\%$ and $\sigma_E/\langle E \rangle$ logically depend on N and σ_z . Variations of ϕ_{RF} by $\pm 1^\circ$ and of σ_z by ± 0.02 mm w.r.t. values of Table 2 do not degrade the energy spread by more than a factor 2.

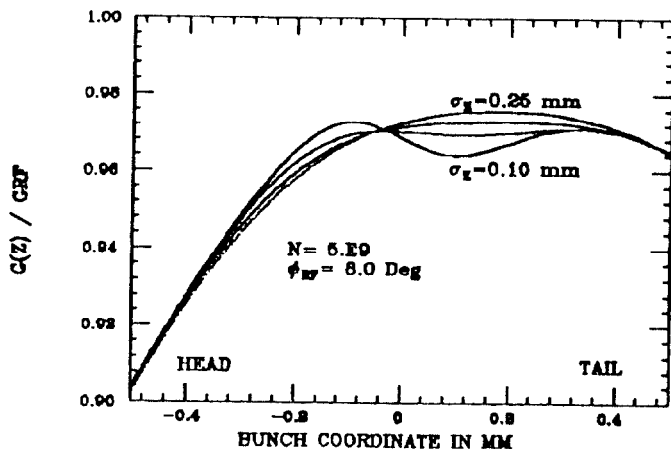


Figure 2. Gradient dependence on bunch length

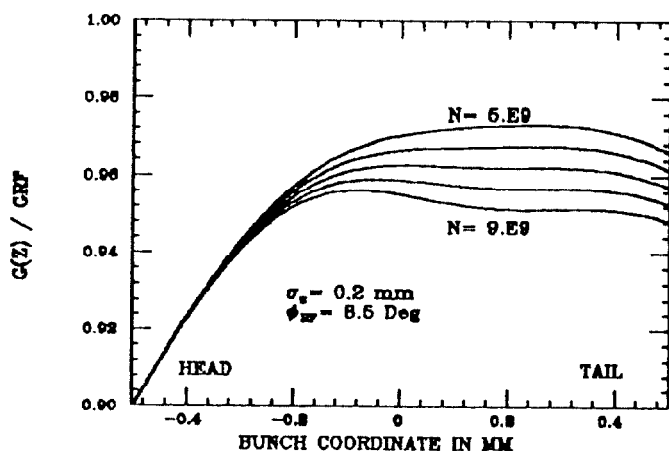


Figure 3. Gradient dependence on bunch charge

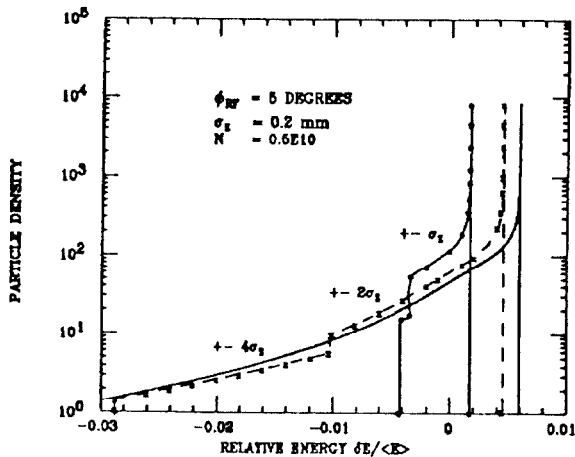


Figure 4. Energy distributions for $\pm 1, 2$ and $4\sigma_z$ cuts.

IV RESULTS AND CONCLUSIONS

With the initial values of $\sigma_z = 0.2$ mm and $N = 5 \cdot 10^9$, the optimum phase lies between 4° and 5° (Fig.1) according to the part of the distribution that contributes to luminosity ($\pm\sigma_z, \pm 2\sigma_z, \pm 4\sigma_z$). The energy distributions behave as in Fig. 4. Only the case with $\pm\sigma_z$ is fully compatible with FF acceptance. Turning to the cases $N = 5 \cdot 10^9$ and $6 \cdot 10^9$ of

Table 2, the distributions have the shape given in Fig. 5, the 3 peaks corresponding to the local maxima and minimum of $G(z)$ and the dense part being well inside the FF acceptance. Since one needs an intensity of at least $5 \cdot 10^9$ at the final focus to reach a luminosity of $10^{33} \text{cm}^{-2} \text{s}^{-1}$ and there is a minimum of σ_E in Table 2, an optimum set of parameters is given by the case $N = 6 \cdot 10^9$ (including the 15% fraction lost). After tracking through the FF system [5], with aberrations and pinch effect, a consistent set of parameters could be found to achieve the required luminosity. The resulting list of tentative parameters is given in Table 3.

Parameters	Values	Units
Energy	1.0	TeV
Luminosity	$\sim 1.1 \cdot 10^{33}$	$\text{cm}^{-2} \text{s}^{-1}$
Enhancement factor	~ 2.4	
Acc. gradient	80	MVm^{-1}
RF frequency	29.985	GHz
Repetition rate	1.7	kHz
Rel. energy loss	0.32	
Critical rel. energy	0.92	
FF Beam ratio	5	
Bunch population	$6 \cdot 10^9$	
V-emittance (γ_e)	$0.5 \cdot 10^{-6}$	rad m
H-emittance (γ_e)	$1.5 \cdot 10^{-6}$	rad m
FF Beam height	12	nm
Bunch length	0.17	mm
FF Beta-function (β_y)	0.576	mm

Table 3 : Main Linac tentative parameters

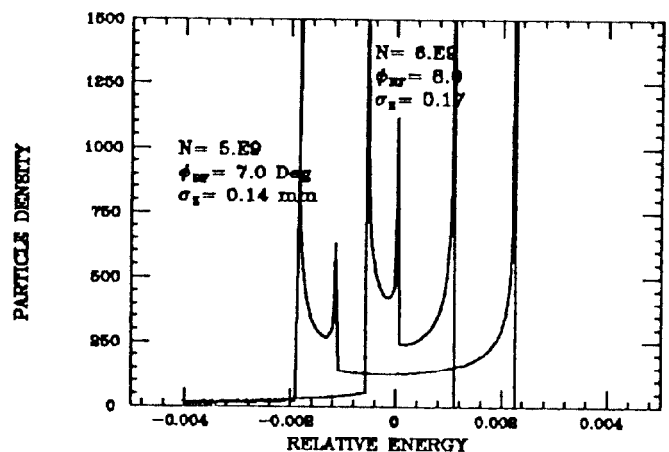


Figure 5. Energy distributions minimizing $\sigma_E / \langle E \rangle$.

V REFERENCES

- [1] W. Schnell, CERN, private communication.
- [2] C. Fischer and G. Guignard, "Energy Spread Compensation in CLIC", CERN-SL/90-122, 1990.
- [3] K.L.F Bane, "Optimizing the average longitudinal phase of the beam in the SLC linac", SLAC-AP-76, 1989.
- [4] H. Henke, "Transverse Damping in a 30 GHz high energy linac", Proc. IEEE PAC 87, 1346, 1987.
- [5] O. Napoly, T. Taylor, B. Zotter, this Conference.